SOLIDS
Electronic Properties

The Energy Band Structure and Optical Spectra of FeBO₃ Calculated with Allowance for Strong Electron Correlations

S. G. Ovchinnikov* and V. N. Zabluda

Kirensky Institute of Physics, Siberian Division, Russian Academy of Sciences, Krasnoyarsk, 660036 Russia
*e-mail: sgo@iph.krasn.ru
Received May 16, 2003; in final form, September 19, 2003

Abstract—A model of the energy band structure of iron borate (FeBO₃) is proposed that combines a one-electron description of the sp states of boron and oxygen with a many-electron description of the d states of iron. The Green functions of d electrons are calculated using the exact Lehmann spectral representation. The energies of the d-type quasiparticles are calculated using terms of the d^4, d^5, and d^6 electron configurations. The optical absorption spectrum of FeBO₃ is determined by local excitons and by the electron excitations with charge transfer. The latter excitations control the nature of the dielectric gap in FeBO₃ crystals. The model parameters are determined from a comparison to the exciton energies. The density of single-particle states in FeBO₃ is calculated. The main bands in the calculated optical absorption spectrum agree well with experimental data for energies up to 3 eV. © 2004 MAIK "Nauka/Interperiodica".

1. INTRODUCTION

Iron borate FeBO₃ is one of a few magnets combining transparency in the visible spectral range with spontaneous magnetization at room temperature. This is a weak ferromagnet with nearly antiparallel spin sublattices of Fe^{3+} ions in the (111) base plane at temperatures below the Néel temperature $T_N = 348$ K [1]. The FeBO₃ crystals possess a calcite structure belonging to the space group $R\bar{3}c$ (D_{3d}^6) [1, 2], in which Fe^{3+} ions are surrounded by an oxygen octahedron of an almost cubic symmetry; bond lengths: Fe–O, 2.028 Å and Fe–Fe, 3.601 Å; O–Fe–O bond angles, 91.82° and 88.18° [3]. Under normal ambient conditions, FeBO₃ is an insulator with a fundamental absorption edge at $E_g^{(0)} = 2.9$ eV [4]. Despite many years of research, there has been permanent interest in studying the properties of FeBO₃ crystals. Recent investigations revealed a structural phase transition in FeBO₃ [5], a collapse of the magnetic moment of Fe^{3+} ions under pressure [6], peculiarities in the concentration dependence of the magnetic and optical properties of some solid solutions of the $V_x Fe_{1-x} BO_3$ system [7], and the light-induced breakage of the magnetic order under conditions of pulsed optical pumping [8].

At the same time, relationships between the observed properties and the electron structure of FeBO₃ have not yet been established even on a qualitative level. There are difficulties in application of the standard band theory to FeBO₃, which are related to strong electron correlations involving the d electrons of iron.

Indeed, a one-electron approach to the d^5 electron configuration of Fe^{3+} ion leads to a partly filled band and the metallic state. In the Hubbard model with strong electron correlations, whereby $U \gg W$ (U is the Coulomb interaction parameter and W is the width of a half-filed d band), we obtain an antiferromagnetic state of the Mott–Hubbard dielectric. However, in FeBO₃ (as well as in many other real substances), a simple pattern based on the Hubbard model is complicated by the presence of a large number of $d(f)$ orbitals.

This paper proposes a many-electron model taking into account all d orbitals and strong electron correlations involving d electrons. Within the framework of this model, the density of single-particle states of d electrons contains contributions due to local quasiparticles with energies

$$\Omega_{ij} = E_i(d^{n+1}) - E_j(d^n),$$

where $E_i(d^n)$ denotes the ith term of the d^n configuration. In the case of FeBO₃, the energies of both high-spin and various low-spin terms of Fe^{2+}, Fe^{3+}, and Fe^{4+} ions become significant. An analogous approach was employed in the analysis of magnetism in d metals [9, 10] and layered cuprates [11]. The model parameters are determined from a comparison to the energies of exciton peaks in the optical absorption spectrum. The calculated density of single-particle states, $N(E)$, is compared to the experimental absorption spectrum in a broad range of energies $E \leq 3$ eV.

The paper is organized as follows. Section 2 describes the proposed many-electron multiband model of FeBO$_3$. Section 3 is devoted to calculation of the local Green functions of d electrons, which is compared to the exact Lehmann spectral representation. Section 4 considers the experimental absorption spectrum of FeBO$_3$ measured in a broad energy range. Section 5 compares the calculated density of states $N(E)$ to the experimental absorption spectra. Finally, in Section 6 we will discuss the temperature dependence of these spectra.

2. A MANY-ELECTRON MULTIBAND MODEL OF THE ELECTRON STRUCTURE OF FeBO$_3$

The *ab initio* one-electron energy band calculations performed for FeBO$_3$ using the density functional method in the local spin density approximation [12] and the generalized gradient approximation [13], together with the calculation of molecular orbitals of a FeB$_6$O$_6$ cluster [7], revealed the following electron structure of FeBO$_3$. The empty conduction band ε_c consists predominantly of the s and p states of boron. The top of the valence band ε_v is formed mostly by the s and p states of oxygen. The energy gap E_{g0} between valence and conduction bands in the antiferromagnetic phase amounts to 2.5 eV [12], which is quite close to the fundamental absorption edge (E_{g0} = 2.9 eV). The band of d electrons occurs at the top of the valence band, and the crystal field parameter is $\Delta \approx 1$ eV [12]. The degree of hybridization of the d electrons of iron with the s and p electrons of oxygen is very small [7, 12], much smaller as compared to the case of $3d$ metal oxides. This is related to a very strong hybridization inside the BO$_3$ group, where the (BO$_3$)$^{3-}$ ion does in fact exist and the electron orbitals of oxygen are closed to boron (which accounts for the small p–d hybridization). This circumstance significantly simplifies the many-electron model, for which the d^n (n = 4, 5, 6) terms of iron in the crystal field can be calculated, rather than the terms of a metal–oxygen complex (as in copper oxides [11]).

The intraatomic part of the Hamiltonian for d electrons can be written as

$$H_{at} = \sum_{\lambda,\sigma}\left(\varepsilon_\lambda n_{\lambda\sigma} + \frac{U_\lambda}{2}n_{\lambda\sigma}n_{\lambda\bar\sigma}\right)$$
$$+ \sum_{\substack{\lambda,\lambda'\\(\lambda\neq\lambda')}}\sum_{\sigma,\sigma'}(V_{\lambda\lambda'}n_{\lambda\sigma}n_{\lambda'\sigma'} - J_{\lambda\lambda'}a^\dagger_{\lambda\sigma}a_{\lambda\sigma'}a^\dagger_{\lambda'\sigma'}a_{\lambda'\sigma}),$$

(1)

where $n_{\lambda\sigma} = a^\dagger_{\lambda\sigma}a_{\lambda\sigma}$, $a_{\lambda\sigma}$ is the operator of d electron creation on one of the five orbitals λ with the spin projection σ ($\bar\sigma = -\sigma$). The first term in (1) describes the atomic d levels in the crystal field. A small uniaxial

component of the crystal field is ignored and it is assumed that

$$\varepsilon(t_{2g}) = \varepsilon_d - 2\Delta/5, \quad \varepsilon(e_g) = \varepsilon_d + 3\Delta/5.$$

The other terms in Hamiltonian (1) represent the Coulomb intraorbital (U_λ) and interorbital ($V_{\lambda\lambda'}$) repulsion and the Hund exchange $J_{\lambda\lambda'}$. For the sake of simplicity, we neglect the orbital dependence of the Coulomb matrix elements, assuming that the three parameters (U, V, and J) are related by the well-known condition $U = 2V + J$.

The kinetic energy of d electrons, as determined by interatomic hopping, is described by the Hamiltonian

$$H_t = \sum_{i,j,\sigma}\sum_{\lambda,\lambda'}t^{\lambda\lambda'}_{ij}a^\dagger_{i\lambda\sigma}a_{j\lambda'\sigma} + \text{H.c.},$$

(2)

where $t^{\lambda\lambda'}_{ij}$ is the matrix element of hopping between ith and jth lattice sites. The main matrix element corresponds to the hops between nearest neighbors: $t \sim t^2_{pd}/|\varepsilon_p - \varepsilon_d|$. However, in view of the weak p–d hybridization between Fe and O atoms, this element is also small, $t \ll U$, which accounts for the strong electron correlation effects. Thus, the model parameters are the two Coulomb integrals, U and J, the crystal field magnitude Δ, the position of the one-electron d level relative to the top of the valence band ε_v ($\delta = \varepsilon_d - \varepsilon_v$), and the hopping integral t. The parameters will be determined by comparison with the experimental optical and photoemission spectra (see Section 4).

The Fe^{3+} ion has a d^5 configuration that can occur in various spin and orbital terms. The considerations below will also imply the knowledge of the terms of d^4 (Fe^{4+}) and d^6 (Fe^{2+}) configurations for description of the hole and electron creation in the many-electron system. The energies of terms in each of these d^n configurations are expressed via the Racah parameters A, B, and C [14, 15]. The B, C and Δ values for the terms of Fe^{3+} ion were determined in [16]: $B = 680$ cm^{-1}, $C = 3160$ cm^{-1}, and $\Delta = 12700$ cm^{-1}.

With neglect of a small uniaxial component of the crystal field, three t_{2g} levels and two e_g levels are degenerate. For the d^5 configuration, the ground state $^6A_1$ (with $S^z = +5/2$) is described by the wave function

$$|d^5, S = 5/2, S^z = 5/2\rangle = t^+_{1\uparrow}t^+_{2\uparrow}t^+_{3\uparrow}e^+_{1\uparrow}e^+_{2\uparrow}|0\rangle,$$
$$E_{5/2}(d^5) = 5\varepsilon_d + 10V - 10J,$$

(3)

where $t^+_{\lambda\sigma}$ (λ = 1, 2, 3) and $e^+_{\lambda\sigma}$ (λ = 1, 2) are the operators of creation of t_{2g} and e_g electrons, respectively, in one of the orbital states λ with the spin projection σ; and $|0\rangle$ is the vacuum state for d electrons. The lowest

excited term $^4T_1$ has a nonzero orbital moment and the spin $S = 3/2$.

The other excited terms with $S = 3/2$ can be written in a similar manner. For example, the term $^4A_1$ has a configuration of $t_{2g}^{3\uparrow}e_g^{\uparrow}e_g^{\downarrow}$ with an energy of

$$E''_{3/2}(d^5) = 5\varepsilon_d + 10V - 6J.$$

The low-spin excited term $^2T_2$ with a configuration of $t_{2g}^{3\uparrow}t_{2g}^{2\downarrow}$ has an energy of

$$E_{1/2}(d^5) = 5\varepsilon_d - 2\Delta + 2U + 8V - 4J.$$

Let us also write the ground and lower excited terms of the d^4 and d^6 configurations. For d^4, the main term ^5E for $S = 2$, $S^z = 2$ has a configuration of $t_{2g}^{3\uparrow}e_g^{\uparrow}$ with an energy of

$$E_2(d^4) = 4\varepsilon_d - 3\Delta/5 + 6V - 6J.$$

In what follows, we will also consider the term $^3T_1$ with $S = 1$ and an energy of

$$E_1(d^4) = 4\varepsilon_d - 8\Delta/5 + U + 5V - 3J$$

and the term $^1E(t_{2g}^{2\uparrow}t_{2g}^{2\downarrow})$ with $S = 0$ and the energy

$$E_0(d^4) = 4\varepsilon_d - 8\Delta/5 + 2U + 4V - 2J.$$

For d^6, the main term $^5T_2$ has a configuration of $t_{2g}^{3\uparrow}t_{2g}^{\downarrow}e_g^{2\uparrow}$ with an energy of

$$E_2(d^6) = 6\varepsilon_d - 2\Delta/5 + U + 14V - 10J,$$

the excited spin triplet $^3T_1$ has an energy of $E_1(d^6)$, and the spin singlet $^1A_1(t_{2g}^{3\uparrow}t_{2g}^{\downarrow})$ has an energy of $E_0(d^6)$. For the given values of B and Δ for each term, the corresponding energies relative to the lowest term of each configuration can be numerically determined using the Tanabe–Sugano diagrams [14, 15] (see Fig. 1 below). Note that a half-occupied d^5 configuration should possess the electron–hole symmetry. This symmetry is revealed when the one-electron energies are measured from the chemical potential level (see Section 5).

3. ONE-PARTICLE GREEN FUNCTION OF d ELECTRONS

For establishing a relationship between many-electron terms and the spectrum of one-particle excitations determining the density of single-particle states, $N(E)$, we use an approach based on the generalization of Hub-
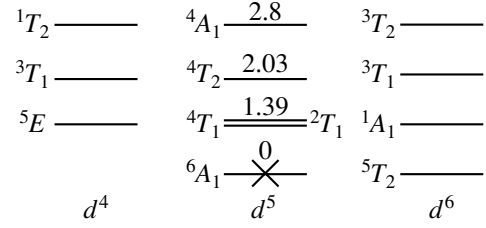
Fig. 1. A diagram of terms for Fe^{4+}, Fe^{3+}, and Fe^{2+} ions in FeBO₃. The cross indicates the occupied lowest sublevel of the term $6A_1$ of Fe^{3+} ion at $T = 0$. Figures at the levels indicate the energies (in eV) relative to the lowest sublevel.

bard's ideas. Since the hops between atoms are small, the exact one-particle Green function $G_{k\sigma}(\omega) = \langle\langle a_{k\sigma}a_{k\sigma}^\dagger\rangle\rangle$ in the zero-order approximation with respect to t reduces to the local function $G^{(0)}(\omega)$. A consistent method for calculating the Green functions at $t/U \ll 1$ is provided by the representation of Hubbard's X operators constructed on the eigenstates of H_{at}. In our case, these are the aforementioned terms of d^n configurations. For the initial Hubbard model without orbital degeneracy, the corresponding perturbation theory has been developed in [17, 18] and the case of arbitrary degeneracy was considered in [19].

The structure of the Green functions of d electrons is revealed by the exact Lehmann spectral representation [20], in which electrons are described as superpositions of various quasiparticles. According to this, for $T = 0$,

$$G_\sigma(k, \omega) = \sum_m \left(\frac{A_m(k, \omega)}{\omega - \Omega_m^+} + \frac{B_m(k, \omega)}{\omega - \Omega_m^-}\right), \quad (4)$$

where the quasiparticle energies are

$$\begin{aligned} \Omega_m^+ &= E_m(N+1) - E_0(N) - \mu, \\ \Omega_m^- &= E_0(N) - E_m(N-1) - \mu, \end{aligned} \quad (5)$$

and their spectral weights are determined by the matrix elements

$$\begin{aligned} A_m(k, \omega) &= |\langle 0, N|a_{k\sigma}|m, N+1\rangle|^2, \\ B_m(k, \omega) &= |\langle m, N-1|a_{k\sigma}|0, N\rangle|^2. \end{aligned} \quad (6)$$

Here, $|m, N\rangle$ denotes the mth many-electron eigenstate of a system with N electrons,

$$H|m, N\rangle = E_m|m, N\rangle,$$

so that index m is essentially the band index numerating quasiparticles possessing the spin $1/2$, the charge e (as

seen in the matrix elements), the energy Ω_m^+ (Ω_m^-), and the spectral weight A_m (B_m).

At a finite temperature, Lehmann's representation can be written, for example, for the retarded Green function (see [21, 22]),

$$G_\sigma^R(k, \omega) = \sum_{m, n} W_n \frac{A_{mn}(k, \omega)}{\omega - \Omega_{mn}^+ + i0} \qquad (7)$$
$$\times [1 + \exp(-\Omega_{mn}^+/T)],$$

where $\Omega_{mn}^+ = E_m(N + 1) - E_n(N) - \mu$ and W_n is the statistical weight of state $|n\rangle$ determined by the Gibbs distribution with the thermodynamic potential Ω:

$$W_n = \exp(\Omega - E_n + \mu N)/T.$$

At $T \neq 0$, both the ground state $|0, N\rangle$ and excited states $|n, N\rangle$ are populated. In this case, quasiparticles are denoted by two indices, m and n, and are considered as excitations in a many-electron system, whereby electron added to the N-electron system in the state $|n, N\rangle$ induces a transition to the final $(N + 1)$-electron state $|m, N + 1\rangle$.

In Lehmann's representation, $|m, N\rangle$ is the unknown state of the whole crystal. As will be shown below, the same structure is inherent in the local Green function $G^{(0)}$ according to the generalized tight binding method [19]. This function is determined by the local many-electron terms $|m, N\rangle$ obtained in Section 2. In the case of $FeBO_3$, significant contributions result from the terms with $N = 4$, 5, and 6. Denoting $|m, N\rangle \equiv |p\rangle$, we define Hubbard's X operator at site f as

$$X_f^{pq} = |p\rangle\langle q| = |mN\rangle\langle m'N'|. \qquad (8)$$

In standard writing, X operators appear with cumbersome notation indicating the initial and final states. In order to simplify this notation, we will use the idea of Zaitsev [17], according to which a pair of indices (p, q) is replaced by the so-called root vector $(p, q) \longleftrightarrow \alpha(p, q) \equiv \alpha$. Since the set of these vectors is denumerable, we introduce the numeration $\alpha \longleftrightarrow \alpha_n$ and then indicate only the number n of the root vector:

$$X_f^{pq} \longleftrightarrow X_f^{\alpha(p, q)} \longleftrightarrow X_f^{\alpha_n} \longleftrightarrow X_f^n.$$

This essentially implies that we construct a table of the correspondence between pairs (p, q), vectors α_n, and indices n necessary for explicitly calculating the commutation relations. Let us define vectors α so as to correspond to the process of electron annihilation, $N_q - N_p = +1$. Then, the operators of electron creation (anni-

hilation) in state $|f\lambda\sigma\rangle$ can be written in the X representation as

$$a_{f\lambda\sigma} = \sum_n \gamma_{\lambda\sigma}(n) X_f^n,$$
$$\qquad\qquad\qquad\qquad\qquad\qquad (9)$$
$$a_{f\lambda\sigma}^\dagger = \sum_n \gamma_{\lambda\sigma}^*(n)(X_f^n)^\dagger,$$

$$\gamma_{\lambda\sigma}(n) = \langle p|a_{f\lambda\sigma}|q\rangle = \langle mN|a_{f\lambda\sigma}|m', N + 1\rangle. \quad (10)$$

Since the Hamiltonian H_{at} in the representation of the Hubbard operators is diagonal, the local Green functions of d electrons are immediately calculated as

$$G_{\lambda\lambda'\sigma}^{(0)}(k, \omega) = \sum_n \gamma_{\lambda\sigma}(n)\gamma_{\lambda'\sigma}^*(n)\frac{F(n)}{\omega - \Omega_n + i0}, \quad (11)$$

where $\Omega_n = E_{m'}(N + 1) - E_m(N)$ is the quasiparticle energy and $F(n) = \langle X_f^{pp}\rangle + \langle X_f^{qq}\rangle$ is the occupation factor. Evidently, the Green functions (11) realize Lehmann's representation inside the unit cell but, in contrast to noncomputable energies and matrix elements in such a representation, all quantities entering into expression (11) can be calculated via the local characteristics of terms. Here, index n numerates quasiparticles with a charge e, spin 1/2, energy Ω_n, and spectral weight $A_{\lambda\lambda'\sigma}(n) = \gamma_{\lambda\sigma}(n)\gamma_{\lambda'\sigma}^*(n)F(n)$. By virtue of completion of the basis set of many-electron states $|p\rangle$, the total spectral weight is the same as that of free electrons.

In the diagram technique developed for X operators [17–19], the series of perturbation theory are constructed for the matrix Green function,

$$D_{nn'}(k, \omega) = \langle\langle X_k^n|(X_k^{n'})^\dagger\rangle\rangle_\omega,$$

rather than for the electron Green function related to the former in the X representation (9) as

$$G_{\lambda\lambda', \sigma}(k, \omega) = \sum_{n, n'} \gamma_{\lambda\sigma}(n)\gamma_{\lambda'\sigma}^*(n')D_{nn'}(k, \omega).$$

It is possible to write a generalized Dyson equation for the Green function $\hat{D}$, in which the perturbation renormalizes both the mass operator and the spectral weight. In the simplest Hartree–Fock approximation, the mass operator is determined as the Fourier transform of the hopping integral $t_{nn'}(k)$. As a result, the dispersion of quasiparticles is described by the following equation:

$$\det\|\delta_{nn'}(\omega - \Omega_n)/F(n) - t_{nn'}(k)\| = 0. \qquad (12)$$

There is an obvious analogy between Eq. (12) and the dispersion equation obtained in the one-electron tight binding method: the structures of these expressions are identical. However, there are important distinctions as well: first, the local energies Ω_n include (unlike the one-electron energies $\varepsilon_{\lambda\sigma}$) intracell Coulomb interactions; second, the band index n of a quasiparticle is determined by a pair of indices of the initial and final states (differing from the band index λ of free electrons); third, the band structure of quasiparticles depends (via the occupation factors $F(n)$) on the density of electrons, temperature, and external fields; and fourth, a one-electron rigid band model cannot be developed for quasiparticles.

For determining the occupation numbers and the factors $F(n)$, it is necessary to solve an equation for the chemical potential. In the X representation, this equation can be written as

$$N_e = \sum_{f, m, N} N \langle X_f^{mN, mN} \rangle, \tag{13}$$

where $\langle X_f^{mN, mN} \rangle$ is the occupation number for the mth term of d^N configuration at the f site. Each term of d^N contributes N electrons to their total number N_e. A solution of this equation for FeBO$_3$ at $T = 0$ appears as

$$\langle X_f^{mN, mN} \rangle = 0$$

for all m and $N \neq 5$, and as

$$\langle X_f^{+5/2, +5/2} \rangle = 1$$

for $N = 5$. For the other d^5 configurations, the occupation numbers are zero. We take into account that, for $S = 5/2$ in a magnetically ordered phase, the term $E_{5/2}(d^5)$ is split with respect to the spin projection and only the lowest sublevel is occupied in each sublattice (+5/2 and –5/2 for sublattices A and B, respectively). Of course, there are zero-point quantum spin fluctuations leading to small population of the sublevels adjacent to $S = 5/2$ ($S^z = 3/2$); this small effect is considered below (see Section 5).

Interatomic hopping in the antiferromagnetic phase is suppressed by the spin–polaron effect [23]. For the hops between nearest neighbors, the effective hopping integral is determined by the product of occupation factors for the two sites belonging to different sublattices (A and B) [24]. For the lowest Hubbard band, the effective hopping Hamiltonian t_v differs from the one-electron integral t,

$$\begin{aligned} t_v^2 = t^2 (\langle X_A^{+5/2, +5/2} \rangle + \langle X_A^{+2, +2} \rangle) \\ \times (\langle X_B^{+5/2, +5/2} \rangle + \langle X_B^{+2, +2} \rangle), \end{aligned} \tag{14}$$

where $\langle X_A^{pp} \rangle$ and $\langle X_B^{pp} \rangle$ are the occupation numbers of state $|p\rangle$ in the sublattices A and B, respectively; $|+5/2\rangle$

and $|+2\rangle$ are the spin sublevels of the terms $E_{5/2}(d^5)$ and $E_2(d^4)$ split with respect to the spin projection in the internal molecular field. For the sublattice A, the level $|+5/2\rangle$ is occupied (being the lowest sublevel), while for the sublattice B (where the lowest level is $|-5/2\rangle$) the level $|+5/2\rangle$ at $T = 0$ is unoccupied. Therefore, for FeBO$_3$ at $T = 0$, $\langle X_B^{+5/2, +5/2} \rangle = 0$ and, hence, the occupation numbers of all d^4 and d^6 sublevels are also zero and the widths of the Hubbard bands are close to zero too.

As a result, it is the poles of the local Green function (11) that determine single-particle contributions of the d-type to $N(E)$. Figure 1 shows the lowest levels of the d^4, d^5, and d^6 configurations (the cross indicates the occupied lowest sublevel of the term $^6A_1$ of the Fe^{3+} ion). Nonzero occupation factors are inherent in the transitions $^6A_1 \longrightarrow d^4$ (hole creation) and $^6A_1 \longrightarrow d^6$ (electron creation), but the matrix elements $\gamma_{\lambda\sigma}(n)$ given by formula (10) are nonzero only when the difference between the spins of terms $|p\rangle$ and $|q\rangle$ is 1/2. In the case under consideration, this implies that nonzero spectral weight and nonzero contribution to the density of states $N(E)$ will be only due to transitions between the lowest terms of all configurations:

$$\begin{aligned} \Omega_v = E_{5/2}(d^5) - E_2(d^4), \\ \Omega_c = E_2(d^6) - E_{5/2}(d^5). \end{aligned} \tag{15}$$

The energy levels Ω_v and Ω_c, or the energy band $\Omega_v(k)$ and $\Omega_c(k)$ appearing with allowance for the weak interatomic hopping are analogs of the lower and upper Hubbard subbands. In addition, it is of interest to consider the quasiparticles for which the matrix element (10) differs from zero, while the spectral weight in the ground state is zero because of zero occupation numbers: such states are referred to as virtual. The virtual states can acquire nonzero weights upon a change in the electron configuration (e.g., in CuO$_2$ layers after hole doping [12]) or upon optical pumping of excited levels. For FeBO$_3$, an example of such a virtual d state is offered by a quasiparticle with an energy of

$$\Omega_v' = E_{3/2}(d^5) - E_2(d^4). \tag{16}$$

For comparison with experiment, it is necessary to determine the model parameters as discussed below. Previously, the optical absorption was studied separately in various spectral intervals. For this reason, the next section is devoted to the experimental absorption spectrum of FeBO$_3$ measured in a broad energy range, $E \leq 3$ eV, covering the entire bandgap width E_{g0}.

4. OPTICAL ABSORPTION SPECTRUM OF FeBO$_3$ IN A BROAD ENERGY RANGE

Previously [25–27], the optical absorption and the magneto-optical Faraday effect in iron borate were
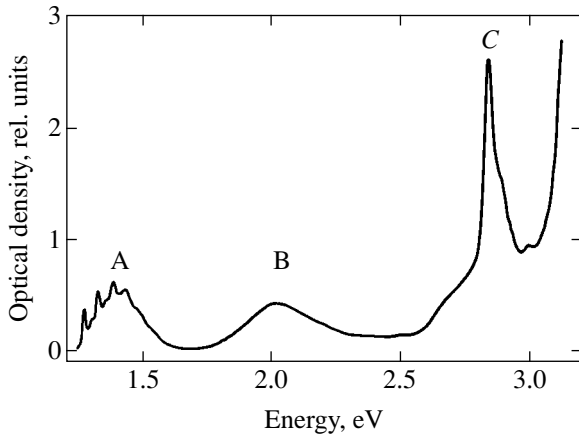
Fig. 2. The optical absorption spectrum of a FeBO$_3$ single crystal measured at 83 K.

studied in the visible and near-infrared (1.0–2.3 eV) spectral range. The results of analogous measurements in the region of strong absorption (2.6–3.3 eV) were reported in [4]. For the sake of convenience, we present the absorption spectrum of FeBO$_3$ measured in a broad energy range.

FeBO$_3$ single crystals were grown by V.V. Rudenko by spontaneous crystallization from solution melt. The crystals had the shape of thin hexahedral plates of a greenish color. The thicknesses of plates selected for the optical measurements were about 80 μm for the former spectral interval and 20 μm for the latter, the sample area in both cases being about 2 mm^2. Orientation of the plates corresponded to the easy magnetization plane, with the hard axis (coinciding with the optical axis of the crystal) being normal to the plate surface. Thus, by applying a small external field parallel to the plane of the crystal, it was possible to readily change the magnetic moment direction in the plane. The optical absorption spectra were measured using an automated spectrometer in a temperature range from 80 to 300 K.

The combination of a high Néel temperature (T_N = 348 K) and transparency in the visible spectral range allows us to perform a detailed comparison of the optical absorption and magneto-optical effects in the transmission mode in the region of three absorption bands wit minimum energies. Our measurements revealed the same three groups of absorption bands (A, B, and C, Fig. 2) as those reported in [4, 25–27]. These bands can be interpreted within the framework of the proposed many-electron model as described below. The main difference of our interpretation consists in that, in addition to the d–d transitions $^6A_{1g}(^6S) \longrightarrow {}^4T_{1g}(^4G)$ (group A), $^6A_{1g}(^6S) \longrightarrow {}^4T_{2g}(^4G)$ (group B), and $^6A_{1g}(^6S) \longrightarrow {}^4A_{1g}$, $^4E_g(^4G)$ (group C), the C band contains contributions due to the p–d transitions with charge transfer. We use the data of Fig. 2 and the X-ray photoelectron spectrum [12] for determining the Coulomb parameters of the model.

Proceeding from expressions for the d–d exciton energies, the parameters of A–C bands, and the additional peaks observed in the Kerr effect in terms of the Racah parameters, it was found [28] that $B = 680$ cm^{-1} and $\Delta \approx 12700$ cm^{-1} for FeBO$_3$; from the same data, we readily obtain $C = 3160$ cm^{-1}. Note that these values of B and C are somewhat lower than the analogous parameters of the free Fe^{3+} ion, but the ratio $C/B = 4.65$ is typical. The crystal field parameter $\Delta = 1.57$ eV is greater as compared to the result ($\Delta = 1$ eV) of the band calculations [12]. Using the known values of B and C, we determine the positions of the lowest excited terms of d^5 configurations with spins 3/2 and 5/2 (see Fig. 1) relative to the ground term $^6A_1$ from the Tanabe–Sugano diagrams [14]. The lowest terms of d^4 and d^6 configurations are also schematically depicted in Fig. 1. Their quantitative characteristics are not presented here because, generally speaking, each d^n configuration has its own level (depending on the chemical potential) from which the energies are measured. Moreover, even determination of the positions of excited terms relative to the lowest term for d^4 and d^6 configuration require knowledge of the corresponding B and Δ values.

Although the energies of these terms will not be required below, we present here for reference the corresponding energies determined from the Tanabe–Sugano diagrams assuming that the B and Δ for F^{4+}, Fe^{3+}, and Fe^{2+} are the same (in eV):

$$\text{Fe}^{4+}: E(^5E) = 0, \quad E(^3T_1) = 0.59, \quad E(^1T_2) = 1.60,$$

$$\text{Fe}^{2+}: E(^5T_2) = 0, \quad E(^1A_1) = 0.17, \quad E(^3T_1) = 0.76,$$

$$E(^3T_2) = 1.18.$$

At the same time, the difference $E(d^{n+1})$–$E(d^n)$ of the energies of these terms has the meaning of energy increment per added electron. A peak at this energy is present on the density of single-particle states $N(E)$. In particular, for the lowest and highest Hubbard subbands, we obtain

$$\Omega_v = \varepsilon_d + 3\Delta/5 + 4V - 4J,$$
$$\Omega_c = \varepsilon_d - 2\Delta/5 + U + 4V. \tag{17}$$

In FeBO$_3$ at $T = 0$, the level Ω_v is filled, while the level Ω_c is empty. This implies that the level Ω_v determines the d-type peak in the experimental X-ray photoelectron spectra or the X-ray absorption spectra. Indeed, such a peak was observed in the X-ray photoelectron spectra at a binding energy of 1.4 eV [12]. Measuring the energies of single-particle states from the top of the valence band ε_v, we set Ω_v–$\varepsilon_v = -1.4$ eV.

As can be seen from the optical absorption spectra, the intensity of peak C is much greater than those of peaks A and B. According to the commonly accepted interpretation of this fact, peak C is formed not only by d–d exciton ($^6A_1 \longrightarrow {}^4A_1$), but makes a contribution due

to the $p^6d^5 \longrightarrow p^5d^6$ transition with charge transfer. The latter transition, reflecting the formation of a hole at the top of the valence band and the filling of level Ω_c, has the energy $\Omega_c - \varepsilon_v = 2.8$ eV. Using the optical data, we can also determine the Hund exchange parameter J. The ground term $^6A_1$ and the excited term $^4A_1$ of the d^5 configuration possess the energies (independent of the crystal field) indicated in Section 2. The difference in these energies, determining the exciton energy for band C (22 600 cm^{-1}), is $E(^4A_1) - E(^6A_1) = 4J$, from which it follows that $J = 5650$ cm$^{-1} = 0.70$ eV. This value of the Hund exchange is typical of $3d$ elements.

5. THE DENSITY
OF SINGLE-PARTICLE STATES IN FeBO$_3$

A scheme of the density of states obtained for the proposed model is depicted in Fig. 3. The diagram shows empty s and p conduction bands with the bottom of the band ε_c, filled valence s and p bands with the top of the band ε_v, and the bandgap $\varepsilon_c - \varepsilon_v = E_{g0} = 2.9$ eV. Thin solid lines (with neglect of the electron dispersion and damping, described by delta functions) show the energies of local d quasiparticles. With allowance for the spin–polaron suppression of interatomic d–d hopping in the magnetically ordered phase (14), the diagram shows only the local d maxima. A fluctuational contribution to the formation of narrow d bands certainly exists, being estimated as $t_v^2 \sim t^2 n_0$, where n_0 is the concentration of zero-point quantum fluctuations [24]. For a three-dimensional isotropic antiferromagnet, the typical value of $S - \langle S^z \rangle \approx 0.078$ [29] yields $n_0 = 0.03$ and $t_v \approx 0.035$ eV, with the corresponding bandwidth of $2zt_v \approx 0.42$ eV.

The upper filled d band Ω_v (15) is situated below the top of the valence band, while the lower empty d band Ω_c is below the bottom of the conduction band (inside the bandgap). Thus, the dielectric gap is determined by the excitations with charge transfer, $p^6d^5 \longrightarrow p^5d^6$, from the top of the valence band to the conduction Ω_c (charge transfer gap in terms of Zaanen *et al.* [30]. Note that the energy of transitions between lower and upper Hubbard bands,

$$\Omega_c - \Omega_v = E_2(d^6) + E_2(d^4) - 2E_{5/2}(d^5), \qquad (18)$$

can be considered as the effective Coulomb repulsion energy U_{eff}. In the Hubbard model $U_{eff} = U$, but in our case $U_{eff} \neq U$ (because of the orbital effects): $U_{eff} = U + 4J - \Delta$. This parameter (in comparison to the d-band width) determines the character of strong electron correlations in the system studied. The experimental values of Ω_v and Ω_c presented in Section 4 yield $U_{eff} = 4.2$ eV. For $J = 0.7$ eV and $\Delta = 1.57$ eV, we obtain $U = 2.97$ eV and $V = (U-J)/2 = 1.15$ eV.
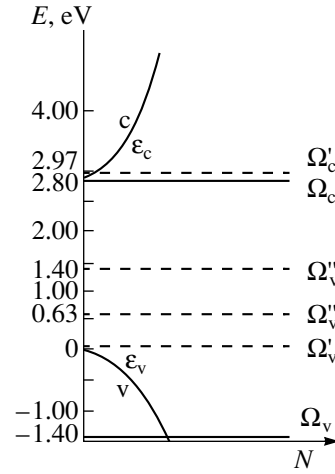
Fig. 3. Schematic diagram of the density of states in a magnetically ordered phase of FeBO$_3$. The Fermi level is situated above the top of the valence band ε_v.

A solution of Eq. (13) for the filled d^5 configuration is the chemical potential occurring between the empty level Ω_c and the filled level Ω_v:

$$\mu = \frac{1}{2}(\Omega_c + \Omega_v) = \varepsilon_d + \frac{U}{2} + \frac{\Delta}{10} + 4V - 2J.$$

Measuring energies relative to the chemical potential clearly reveals the electron–hole symmetry of the system:

$$\Omega_c - \mu = \frac{U}{2} - \frac{\Delta}{2} + 2J = -(\Omega_v - \mu).$$

The spectral weights of states Ω_v and Ω_c (with allowance for spin) is unity, rather than two as in the case of free electrons. In the diagram of Fig. 3, primed symbols indicate the virtual levels Ω_v' (16), $\Omega_v'' = E(^4T_2) - E_2(d^4)$, and $\Omega_v'' = E(^4A_1) - E_2(d^4)$. The spectral weight of these levels in the ground state is zero, while the energies of transitions $\Omega_v' - \Omega_v$, $\Omega_v'' - \Omega_v$, and $\Omega_v''' - \Omega_v$ coincide with the exciton energies ε_A, ε_B, and ε_C. Under the conditions of optical pumping of the terms $^4T_1$, $^4T_2$, and $^4A_1$, their populations are no longer zero and the spectral weights of the virtual levels Ω_v', Ω_v'', Ω_v''' are proportional to the concentration of optically excited Fe^{3+} ions. Thus, the exciton transitions inside the same d^n configuration can be represented by a virtual level in the one-electron density of states, and the $\Omega_v \longrightarrow \Omega_v'$ transition corresponds to the appearance of a hole in the band Ω_v and electron in the band Ω'.

Let us consider interpretation of the optical absorption spectrum within the framework of the proposed model. Since the exciton band A was used for determining the model parameters, the coincidence of theoreti-

cal and experimental energies for this band is trivial. At low temperatures, band A exhibits splitting into components A_1–A_4. Line A_1 is interpreted as a magnon satellite of the pure exciton line, and bands A_2–A_4, as magnon repetitions of the exciton–magnon line A_1 [25]. Indeed, at low temperatures, the spin levels $E_S(d^n)$ are split by the internal molecular field $I\langle S^z \rangle$ with respect to the spin projection M_z:

$$E_S(d^n, M_z) = E_S(d^n) - I\langle S^z \rangle M_z. \quad (19)$$

At $T = 0$, only the sublevel $M_z = +5/2$ of the term $^6A_1$ is occupied, so that transitions to the lower sublevel $M_z = +5/2$ of the $^4T_1$ term require the participation of a magnon.

As for the peak B, this absorption band corresponds to the exciton with $\varepsilon_B = E(^4T_2)-E(^6A_1)$. The band C contains contributions due to exciton $\varepsilon_C = E(^4A_1)-E(^6A_1)$ and due to transitions from the top of the valence band to the bands Ω_c (excitation with charge transfer).

6. TEMPERATURE DEPENDENCE OF THE INTENSITY OF BAND A

The temperature dependence of the band structure of local quasiparticles is revealed by general formula (7) showing temperature blurring of the distribution function. However, magnetic materials exhibit a stronger dependence due to interrelated electron and magnetic subsystems. All the absorption lines A_1–A_4 shift by 40 cm^{-1} toward lower energies when the temperature increases in the range from 30 to 200 K [28]. For the A_1 component, relation (19) yields

$$\Delta E(T) = E_{5/2}(d^5, +5/2) - E_{3/2}(d^5, +3/2)$$
$$= \Delta E(0) + I\langle S^z \rangle.$$

As the temperature T grows, the value of $\langle S^z \rangle$ decreases so that ΔE shifts toward smaller energies. The results of measurements of the sublattice magnetization $\langle S^z \rangle(T)$ [31] show that

$$\frac{\langle S^z \rangle(30 \text{ K}) - \langle S^z \rangle(200 \text{ K})}{\langle S^z \rangle(30 \text{ K})} \approx \frac{1}{8}.$$

Using this estimate and the shift of exciton A_1,

$$\Delta E(30 \text{ K}) - \Delta E(200 \text{ K}) \approx \frac{5}{2}I \times \frac{1}{8},$$

it is possible to evaluate the Fourier transform of the interatomic exchange integral for $q = 0$ as $I \approx 0.015$ eV. This value determines the Néel temperature and, in the simplest variant of the mean field approximation,

$$T_N = IS(S + 1)/3.$$

This yields $T_N = 317$ K, which is quite close to the experimental value of $T_N = 348$ K. We can also relate the magnetic and electron parameters by assuming that $I = Jz$, where J is the indirect exchange interaction between neighboring Fe^{3+} ions. Estimating this quantity as

$$J \sim 2t_v^2/U_{\text{eff}},$$

we obtain $t_v \approx 0.05$ eV. In Section 4, the fluctuation contribution was estimated as $t_v \approx 0.035$ eV. Therefore, the electron, magnetic, and optical properties of $FeBO_3$ in the proposed model exhibit a sufficiently good mutual agreement.

7. CONCLUSIONS

A question can arise as to how correct are the results of one-electron energy band calculations [12, 13] and can these results be applied to a system such as $FeBO_3$ with electron–spin correlations. Indeed, calculations [12] performed in the approximation of the local spin density functional ignore the correlation effects. As a result, the Fermi level falls within a partly occupied d band that implies the metallic state. Calculations [13] performed in the generalized gradient approximation take into account nonlocal corrections to the density functional, although it is not clear whether this approach adequately describes the regime of strong electron correlations. Nevertheless, the antiferromagnetic phase exhibits a dielectric state [13]. The calculation of pressure-induced changes in the magnetic state also rather well reproduces the magnetic and structural phase transitions observed recently [5, 6].

We believe that the results of band calculations in the local density functional approximation can be used as the initial information that should be supplemented by corrections for the transition from one-electron description of d electrons to local quasiparticles–excitations between d^n and d^{n+1} terms. There are no reasons for not believing the results of band calculations for the s and p states of boron and oxygen. The bandgap width $E_g^{(0)}$ is close to the experimental value, the crystal field Δ is 1.5 times the value according to the band theory, and the d band width in this theory is significantly overestimated.

On the other hand, it is by no means possible to use the level positions and occupation statistics obtained for the one-electron d band. The strong electron correlations not only split the d band into Hubbard's subbands, but (even more importantly) change the statistics of quasiparticles of the d type. As was demonstrated above, this gives rise to very unusual virtual states with the spectral weights determined by the nonstoichiometry or the incident light intensity.

Recently, [32], we interpreted the phase transition under pressure in $FeBO_3$ within the framework of the same model as being due to the intersection of the levels of terms $^6A_1$ and $^4T_2$ caused by increasing crystal field Δ. The model parameters in [32] were partly deter-

mined using the results of band calculations [12] and partly based on the optical data. Subsequently, it was established that this approach can lead to ambiguous results, since the theoretical and experimental values of the same quantity are not independent. In this study, we have used only experimental data for determining the model parameters. As a result, the values of $U \approx 3$ eV and $J \approx 0.7$ eV have proved to be much greater than those obtained in [32]. However, the conclusions [32] concerning the nature of the phase transition in $FeBO_3$ under pressure remain fully valid.

To summarize, we have constructed a many-electron model of the band structure of $FeBO_3$ taking into account both the one-electron s and p states of boron and oxygen and many-electron terms of Fe^{2+}, Fe^{3+}, and Fe^{4+} ions formed under the conditions of strong intraatomic d–d correlations. The density of one-electron states exhibits a set of narrow peaks related to local quasiparticles of the d type on the background of valence and conduction bands. Each quasiparticle corresponds to an electron with charge e, spin 1/2, and a reduced spectral weight. Only the sum of the spectral weights of all quasiparticles gives the one-electron spectral weight. Using this approach, it is possible to identify, with good fit to experiment, the main features of the absorption spectrum of $FeBO_3$ related both to excitons and the electron excitations with charge transfer. The parameters of electron and magnetic structures are also well consistent.

REFERENCES

1. R. Wolff, A. J. Kurtzig, and R. C. Lecraw, J. Appl. Phys. **41**, 1218 (1970).

2. I. Bernal, C. W. Struck, and J. G. White, Acta Crystallogr. **16**, 849 (1963).

3. R. Diehl, Solid State Commun. **17**, 743 (1975).

4. I. S. Édel'man, A. V. Malakhovskiĭ, T. I. Vasil'eva, and V. N. Seleznev, Fiz. Tverd. Tela (Leningrad) **14**, 2810 (1972) [Sov. Phys. Solid State **14**, 2442 (1972)].

5. A. G. Gavriliuk, I. A. Trojan, R. Boehler, *et al.*, Pis'ma Zh. Éksp. Teor. Fiz. **75**, 25 (2002) [JETP Lett. **75**, 23 (2002)].

6. V. A. Sarkisyan, I. A. Troyan, M. S. Lyubutin, *et al.*, Pis'ma Zh. Éksp. Teor. Fiz. **76**, 788 (2002) [JETP Lett. **76**, 664 (2002)].

7. N. B. Ivanova, V. V. Rudenko, A. D. Balaev, *et al.*, Zh. Éksp. Teor. Fiz. **121**, 354 (2002) [JETP **94**, 299 (2002)].

8. A. V. Kimel, R. V. Pisarev, J. Hohlfeld, and Th. Rasing, Phys. Rev. Lett. **89**, 287401 (2002).

9. R. O. Zaĭtsev, Pis'ma Zh. Éksp. Teor. Fiz. **65**, 881 (1997) [JETP Lett. **65**, 925 (1997)].

10. R. O. Zaĭtsev, Pis'ma Zh. Éksp. Teor. Fiz. **72**, 109 (2000) [JETP Lett. **72**, 77 (2000)].

11. V. A. Gavrichkov, S. G. Ovchinnikov, A. A. Borisov, and E. G. Goryachev, Zh. Éksp. Teor. Fiz. **118**, 422 (2000) [JETP **91**, 369 (2000)].

12. A. V. Postnikov, St. Bartkowski, M. Neumann, *et al.*, Phys. Rev. B **50**, 14849 (1994).

13. K. Parlinski, Eur. Phys. J. B **27**, 283 (2002).

14. Y. Tanabe and S. Sugano, J. Phys. Soc. Jpn. **9**, 766 (1954).

15. D. T. Sviridov and Yu. F. Smirnov, *Theory of Optical Spectra of Transition-Metal Ions* (Nauka, Moscow, 1977).

16. I. S. Édel'man and A. V. Malakhovskiĭ, Fiz. Tverd. Tela (Leningrad) **15**, 3084 (1973) [Sov. Phys. Solid State **15**, 2056 (1973)].

17. R. O. Zaĭtsev, Zh. Éksp. Teor. Fiz. **70**, 1100 (1976) [Sov. Phys. JETP **43**, 574 (1976)].

18. Yu. A. Izyumov, M. I. Katsnel'son, and Yu. N. Skryabin, *Magnetism of Collectivized Electrons* (Fizmatgiz, Moscow, 1994).

19. V. V. Val'kov and S. G. Ovchinnikov, *Quasi-Particles in Strongly Correlated Systems* (Sib. Otd. Ross. Akad. Nauk, Novosibirsk, 2001).

20. H. Lehmann, Nuovo Cimento **11**, 342 (1954).

21. A. A. Abrikosov, L. P. Gor'kov, and I. E. Dzyaloshinskiĭ, *Methods of Quantum Field Theory in Statistical Physics* (Fizmatgiz, Moscow, 1962; Prentice Hall, Englewood Cliffs, N.J., 1963).

22. E. M. Lifshitz and L. P. Pitaevskiĭ, *Course of Theoretical Physics*, Vol. 5: *Statistical Physics* (Nauka, Moscow, 1978; Pergamon, New York, 1980), Part 2.

23. É. L. Nagaev, *Physics of Magnetic Semiconductors* (Nauka, Moscow, 1979).

24. S. G. Ovchinnikov, Zh. Éksp. Teor. Fiz. **107**, 796 (1995) [JETP **80**, 451 (1995)].

25. B. Andlauer, O. F. Schirmer, and J. Schneider, Solid State Commun. **13**, 1655 (1973).

26. A. J. Kurtzig, R. Wolff, R. C. Le Graw, and J. W. Nielsen, Appl. Phys. Lett. **14**, 350 (1969).

27. K. Egashira, T. Manabe, and H. Katsiraki, J. Phys. Soc. Jpn. **31**, 602 (1971).

28. A. V. Malakhovskii and I. S. Edelman, Phys. Stat. Sol. **B74**, K145 (1976).

29. P. W. Anderson, Phys. Rev. **86**, 694 (1952).

30. J. Zaanen, G. A. Sawatzky, and J. W. Allen, Phys. Rev. Lett. **55**, 418 (1985).

31. A. M. Kadomtseva, R. Z. Levitin, Yu. F. Popov, *et al.*, Fiz. Tverd. Tela (Leningrad) **14**, 214 (1972) [Sov. Phys. Solid State **14**, 172 (1972)].

32. S. G. Ovchinnikov, Pis'ma Zh. Éksp. Teor. Fiz. **77**, 808 (2003)[JETP Lett. **77**, 676 (2003)].

Translated by P. Pozdeev